

Five-Coordinate Iron(III) Porphycenes:  $^1\text{H}$  NMR, Magnetic, and Structural StudiesKrystyna Rachlewicz,<sup>†</sup> Lechosław Latos-Grażyński,<sup>\*,†</sup> Emanuel Vogel,<sup>‡</sup> Zbigniew Ciunik,<sup>†</sup> and Lucjan B. Jerzykiewicz<sup>†</sup>

Department of Chemistry, University of Wrocław, 14 F. Joliot-Curie Street, Wrocław 50 383, Poland, and Institut für Organische Chemie, Universität zu Köln, Greinstrasse 4, D-50939 Köln, Germany

Received July 9, 2001

Five-coordinate iron(III) 2,7,12,17-tetrapropylporphycene (TPrPc)Fe<sup>III</sup>X (X = C<sub>6</sub>H<sub>5</sub>O<sup>-</sup>, Cl<sup>-</sup>, Br<sup>-</sup>, I<sup>-</sup>, ClO<sub>4</sub><sup>-</sup>) complexes have been investigated. The  $^1\text{H}$  NMR spectra demonstrate downfield shifts for pyrrole resonances [(TPrPc)Fe<sup>III</sup>-(C<sub>6</sub>H<sub>5</sub>O), 65.3 ppm; (TPrPc)Fe<sup>III</sup>Cl, 28.5 ppm] but large upfield ones for (TPrPc)Fe<sup>III</sup>Br (-7.8 ppm), (TPrPc)Fe<sup>III</sup>I (-49.4 ppm), and (TPrPc)Fe<sup>III</sup>ClO<sub>4</sub> (-77.1 ppm) (294 K, CD<sub>2</sub>Cl<sub>2</sub>). The pyrrole chemical shifts span the remarkable +70 to -80 ppm range. The variable-temperature  $^1\text{H}$  NMR spectra of (TPrPc)Fe<sup>III</sup>X demonstrate anti-Curie behavior with a sign reversal for (TPrPc)Fe<sup>III</sup>Cl. These behaviors are consistent with the admixed  $S = 3/2$ ,  $5/2$  ground electronic state with a dominating contribution of the  $S = 3/2$  one. In terms of the chemical shift, (TPrPc)Fe<sup>III</sup>(ClO<sub>4</sub>) can be considered as an example of the purest  $S = 3/2$  state in the investigated series. The extent of the  $S = 5/2$  contribution in the admixed  $S = 3/2$ ,  $5/2$  ground electronic state, as gradated solely the basis of the pyrrole proton paramagnetic shifts, is controlled by the strength of the axial ligand, following the magnetochemical series (Evans, D. R.; Reed, C. A. *J. Am. Chem. Soc.* **2000**, *122*, 4660). Significantly iron(III) 2,7,12,17-tetrapropylporphycene, soluble in typical organic solvents, can be considered as a universal framework to classify the ligand strength in a magnetochemical series, consistently using the  $\beta$ -H pyrrole paramagnetic shifts as a fundamental criterion. The structure of (TPrPc)Fe<sup>III</sup>Cl has been determined by X-ray crystallography. The iron is five-coordinate with bonds of nearly equal length to the four pyrrole nitrogen atoms (Fe-N in the range 1.983(5)–2.006(6) Å). The iron lies 0.583(1) Å out of the mean plane of the macrocycle and 0.502(5) Å out of the mean N<sub>4</sub> plane. In the solid, pairs of molecules are positioned about the center of symmetry so there is face-to-face  $\pi$ - $\pi$  contact. The mean plane separation is 3.38 Å, and the lateral shift of the porphycene center along the Fe-N bond is 4.490 Å. The distance from one porphycene center to the other is 5.62 Å, and the iron-iron separation is 6.304(2) Å.

## Introduction

Porphyrin isomers, which emerged in the past decade, porphycene,<sup>1</sup> corrophycene,<sup>2,3</sup> hemiporphycene,<sup>4,5</sup> isoporphycene,<sup>6</sup> and inverted porphyrin (2-aza-21-carbaporphyrin),<sup>7,8</sup> offer particularly interesting perspectives in alternation and control of metalloporphyrin properties.<sup>9,10</sup> In this respect one takes into account the notable changes of their coordinating (NNNN) tetragon geometry.

\* To whom correspondence should be addressed. E-mail: LLG@wchuw.chem.uni.wroc.pl.

<sup>†</sup> University of Wrocław.

<sup>‡</sup> Universität zu Köln.

- (1) Vogel, E.; Köcher, M.; Schmickler, H.; Lex, J. *Angew. Chem., Int. Ed. Engl.* **1986**, *25*, 257.
- (2) Sessler, J. L.; Brucker, E. A.; Weghorn, S. J.; Kisters, M.; Schäfer, M.; Lex, J.; Vogel, E. *Angew. Chem., Int. Ed. Engl.* **1994**, *33*, 2308.
- (3) Aukauloo, M. A.; Guillard, R. *New J. Chem.* **1994**, *18*, 1205.
- (4) Vogel, E.; Bröring, M.; Weghorn, S. J.; Scholz, P.; Deponte, R.; Lex, J.; Schmickler, H.; Schaffner, K.; Braslavsky, S. E.; Müller, M.; Pörting, S.; Fowler, C. J.; Sessler, J. L. *Angew. Chem., Int. Ed. Engl.* **1997**, *36*, 1651.

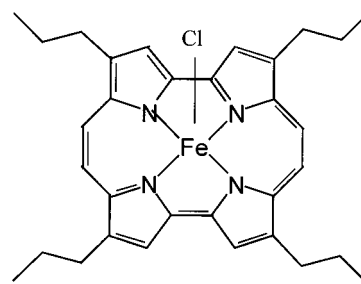
- (5) Callot, H. J.; Rohrer, A.; Tschamber, T.; Metz, B. *New J. Chem.* **1995**, *19*, 155.
- (6) Vogel, E.; Bröring, M.; Erben, C.; Demuth, R. *Angew. Chem., Int. Ed. Engl.* **1997**, *36*, 353.
- (7) Chmielewski, P. J.; Latos-Grażyński, L.; Rachlewicz, K.; Głowiak, T. *Angew. Chem., Int. Ed. Engl.* **1994**, *33*, 779.
- (8) Furuta, H.; Asano, T.; Ogawa, T. *J. Am. Chem. Soc.* **1994**, *116*, 767.
- (9) Sessler, J. L.; Weghorn, S. J. *Expanded, Contracted and Isomeric Porphyrins*; Pergamon Tetrahedron Organic Chemistry Series, Vol. 15; Elsevier Science: Oxford, U.K., 1997.
- (10) Sessler, J. L.; Gebauer, A.; Vogel, E. *Porphyrin Isomers*. In *The Porphyrin Handbook*; Kadish, K. M., Smith, K. M., Guillard, R., Eds.; Academic Press: New York, 2000; Vol. 2, p 1.

Previously, some similarities between metalloporphycenes and the corresponding metalloporphyrins have been established.<sup>9,10</sup> In iron(III) porphycene (PcFe<sup>III</sup>) chemistry, the following series of complexes were reported: PcFe<sup>III</sup>X (X = Cl<sup>-</sup>, Br<sup>-</sup>, N<sub>3</sub><sup>-</sup>, CH<sub>3</sub>COO<sup>-</sup>, CF<sub>3</sub>COO<sup>-</sup>, C<sub>6</sub>H<sub>5</sub>O<sup>-</sup>),<sup>11,12</sup> [(PcFe<sup>III</sup>)<sub>2</sub>O],<sup>13,14</sup> PcFe<sup>III</sup>R, (R = aryl ligands),<sup>15,16</sup> and [PcFe-(THF)<sub>2</sub>]ClO<sub>4</sub>.<sup>17</sup> Using electrochemistry and spectroelectrochemistry, it has been demonstrated that porphycene stabilizes high oxidation states of iron in the following systems: [(Pc•)Fe<sup>III</sup>]<sup>2+</sup>,<sup>18</sup> [PcFe<sup>IV</sup>R]<sup>+</sup>,<sup>19</sup> and {[PcFe<sup>IV</sup>]<sub>2</sub>O}<sup>2+</sup>.<sup>14,18</sup> Iron(II) porphycene, when generated electrochemically, was also found to react spontaneously with dioxygen to give a μ-oxo-bridged diiron(III) species.<sup>18</sup> Introduction of dioxygen into a toluene-*d*<sub>8</sub> solution of (TPrPc)Fe<sup>II</sup> at 203 K resulted in formation of a μ-peroxo diiron(III) porphycene, (TPrPc)-Fe<sup>III</sup>-O-O-Fe<sup>III</sup>(TPrPc).<sup>20</sup> Reaction of (TPrPc)Fe<sup>III</sup>-O-O-Fe<sup>III</sup>(TPrPc) with nitrogen bases (B, pyridine-*d*<sub>5</sub>, 1-methylimidazole) resulted in a homolytic cleavage of the μ-peroxo bridge to form the ferryl porphycene B(TPrPc)Fe<sup>IV</sup>O complex.<sup>20</sup>

The <sup>1</sup>H NMR spectra of paramagnetic metalloporphyrins<sup>21,22</sup> and core-modified metalloporphyrins<sup>23</sup> offer a sensitive probe for distinguishing between the various spin, ligation, and oxidation states of the formed species. Generally, some essential qualitative similarities of the spectroscopic patterns of iron porphyrin and iron porphycenes at each oxidation state have been detected.<sup>12,20</sup> The observed differences could result either from an altered delocalization path or from the modifications of the ground electronic state. Actually both factors may act simultaneously.

In the present paper we have focused on the <sup>1</sup>H NMR characterization of five-coordinate iron(III) 2,7,12,17-tetra-*n*-propylporphycene (TPrPc)Fe<sup>III</sup>X, X = C<sub>6</sub>H<sub>5</sub>O<sup>-</sup>, Cl<sup>-</sup>, Br<sup>-</sup>, I<sup>-</sup>, ClO<sub>4</sub><sup>-</sup> (Chart 1). The β-H pyrrole resonances provided—similarly to the case of iron(III) tetraarylporphyrins—a direct

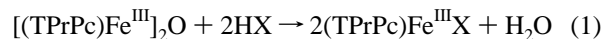
Chart 1



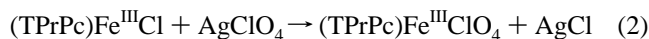
probe of the spin density and/or a ground electronic state. The structural and magnetic susceptibility investigations corroborated the NMR analysis.

## Results

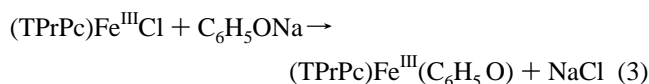
**Synthesis.** A general route to synthesize (TPrPc)Fe<sup>III</sup>X complexes is a cleavage of the μ-oxo derivative [(TPrPc)-Fe<sup>III</sup>]<sub>2</sub>O with the appropriate acid HX (X = Cl<sup>-</sup>, Br<sup>-</sup>, I<sup>-</sup>).<sup>12</sup>



Conversion of the chloride ion to the perchlorate ion was carried out with use of the silver perchlorate.<sup>24,25</sup>



(TPrPc)Fe<sup>III</sup>(C<sub>6</sub>H<sub>5</sub>O) has been obtained in the reaction of (TPrPc)Fe<sup>III</sup>Cl with sodium phenoxide.



**Crystal and Molecular Structure of (TPrPc)Fe<sup>III</sup>Cl.** The structure of (TPrPc)Fe<sup>III</sup>Cl has been determined by X-ray crystallography. The structure displays disorder in the location of the porphycene macrocycle. The positions of iron(III) and the axial chloride are preserved in both forms, but the macrocycles are rotated by 90° with respect to the axis defined by Fe—Cl. The perspective view of the major form is shown in Figure 1.

There is no crystallographically imposed symmetry on the molecule. A selection of important bond distances and angles are reported in Table 1. The iron is five-coordinate with bonds of nearly equal length (Fe—N in the range 1.983(5)—2.006(6) Å) to the four pyrrole nitrogen atoms. The Fe—N distances are slightly shorter than determined for typical five-coordinate high-spin (*S* = 5/2) iron(III) porphyrins.<sup>26–31</sup> These distances are shorter than those observed for highly distorted chloroiron(III) porphyrins.<sup>32–34</sup> In fact these bond lengths are in the range determined for the iron(III) porphyrin with pure *S* = 3/2 or admixed *S* = 3/2, 5/2 spin states.<sup>24,35–40</sup> The corresponding bond distances in chloroiron(III) tetraazaporphyrin (pure *S* = 3/2)<sup>41</sup> and chloroiron(III) phthalocya-

- (11) Gisselbrecht, J. P.; Gross, M.; Köcher, M.; Lausmann, M.; Vogel, E. *J. Am. Chem. Soc.* **1990**, *112*, 8618.
- (12) Lausmann, M.; Zimmer, I.; Lex, J.; Lueken, H.; Wiegardt, K.; Vogel, E. *Angew. Chem., Int. Ed. Engl.* **1994**, *33*, 736.
- (13) Oertling, W. A.; Wu, W.; López-Garriga, J.-L.; Kim, Y.; Chang, C. K. *J. Am. Chem. Soc.* **1991**, *113*, 127.
- (14) Kadish, K. M.; Boulas, P.; D'Souza, F.; Aukauloo, A. M.; Guillard, R.; Lausmann, M.; Vogel, E. *Inorg. Chem.* **1994**, *33*, 471.
- (15) Kadish, K. M.; D'Souza, F.; Van Caemelbecke, E.; Boulas, P.; Vogel, E.; Aukauloo, A. M.; Guillard, R. *Inorg. Chem.* **1994**, *33*, 4474.
- (16) Kadish, K. M.; Tabard, A.; Van Caemelbecke, E.; Aukauloo, A. M.; Richard, P.; Guillard, R. *Inorg. Chem.* **1998**, *37*, 6168.
- (17) Ikeue, T.; Ohgo, Y.; Takahashi, M.; Takeda, M.; Neya, S.; Funasaki, N.; Nakamura, M. *Inorg. Chem.* **2001**, *40*, 3650.
- (18) Bernard, C.; Le Mest, Y.; Gisselbrecht, J. P. *Inorg. Chem.* **1998**, *37*, 181.
- (19) Kadish, K. M.; Tabard, A.; Van Caemelbecke, E.; Aukauloo, A. M.; Richard, P.; Guillard, R. *Inorg. Chem.* **1998**, *37*, 6168.
- (20) Rachlewicz, K.; Latos-Grażyński, L. Vogel, E. *Inorg. Chem.* **2000**, *39*, 3247.
- (21) Walker, F. A.; Simonis, U. *Biological Magnetic Resonance*. In *NMR of Paramagnetic Molecules*; Berliner, L. J., Reuben, J., Eds.; Plenum Press: New York, 1993; Vol. 12, p 133.
- (22) Walker, F. A. Proton NMR Spectroscopy of Paramagnetic Metalloporphyrins. In *The Porphyrin Handbook*; Kadish, K. M., Smith, K. M., Guillard, R., Eds.; Academic Press: New York, 2000; Vol. 5, p 81.
- (23) Latos-Grażyński, L. Core Modified Heteroanalogues of Porphyrins and Metalloporphyrins. In *The Porphyrin Handbook*; Kadish, K. M., Smith, K. M., Guillard, R., Eds.; Academic Press: New York, 2000; Vol. 2 p 361.

- (24) Reed, C. A.; Mashinko, T.; Bentley, S. P.; Kastner, M. E.; Scheidt, W. R.; Spartalian, K.; Lang, G. *J. Am. Chem. Soc.* **1979**, *101*, 2948.
- (25) Nasset, M. J. M.; Cai, S.; Shokhireva, T. Kh.; Shokhirev, N. V.; Jacobson, S. E.; Jayaraj, K.; Gold, A.; Walker, F. A. *Inorg. Chem.* **2000**, *39*, 532.

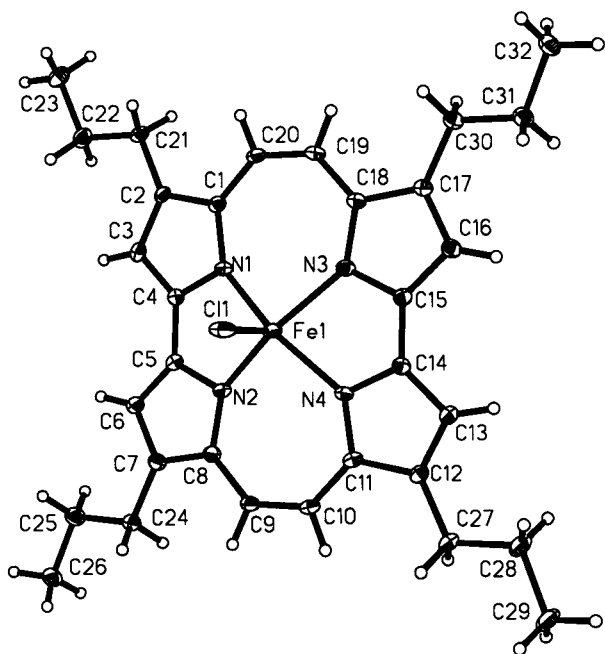


**Figure 1.** Perspective view of (TPrPc)Fe<sup>III</sup>Cl showing 50% thermal countours.

nines (admixed intermediate-spin state) are equal to 1.929 and 1.945 Å, respectively.<sup>42</sup> Importantly the Fe–N bond distances in (TPrPc)Fe<sup>III</sup>Cl are shorter than found for  $\mu$ -oxo diiron(III) porphycene complexes: [(TPrPc)Fe<sup>III</sup>]<sub>2</sub>O, 2.052 Å; [(T(*t*-Bu)Pc)Fe<sup>III</sup>]<sub>2</sub>O, 2.056 Å.<sup>12</sup> The Fe–Cl distance is 2.2508(9) Å, which is typical for chloroiron(III) porphyrins<sup>28,31–34</sup> and resembles that for chloroiron(III) phthalocyanine and chloroiron(III) tetraazaporphyrin.<sup>41,42</sup>

- (26) Phillippi, M. A.; Baenziger, N.; Goff, H. M. *Inorg. Chem.* **1981**, *20*, 3904.
- (27) Gold, A.; Jayaraj, K.; Doppelt, P.; Fischer, J.; Weiss, R. *Inorg. Chim. Acta* **1988**, *150*, 177.
- (28) Scheidt, W. R.; Gouterman, M. Ligands, Spin State, and Geometry in Hemes and Related Metalloporphyrins. In *Iron Porphyrins Part I*; Lever, A. B. P., Gray, H., Eds.; Addison-Wesley: Reading, MA, 1983; p 89.
- (29) Scheidt, W. R.; Lee, Y. *Struct. Bonding (Berlin)* **1987**, *64*, 1.
- (30) Scheidt, W. R.; Finnegan, M. G. *Acta Crystallogr.* **1989**, *C45*, 1214.
- (31) Balch, A. L.; Latos-Grażyński, Noll, B. C.; Olmstead, M. M.; Zovinka, E. *P. Inorg. Chem.* **1992**, *31*, 2248.
- (32) Cheng, R.-J.; Chen, P.-Y.; Gau, P.-R.; Chen, C.-C.; Peng, S.-M. *J. Am. Chem. Soc.* **1997**, *119*, 2563.
- (33) Schünemann, V.; Gerdan, M.; Trautwein, A. X.; Haoudi, N.; Mandon, D.; Fischer, J.; Weiss, R.; Tabard, A.; Guillard, R. *Angew. Chem., Int. Ed.* **1999**, *38*, 3181.
- (34) Mazzanti, M.; Marchon, J.-C.; Wojaczyński, J.; Wołowicz, S.; Latos-Grażyński, L.; Shang, M.; Scheidt, W. R. *Inorg. Chem.* **1998**, *37*, 2476.
- (35) Shelly, K.; Bartzak, T.; Scheidt, W. R.; Reed, C. A. *Inorg. Chem.* **1985**, *24*, 4325.
- (36) Gupta, G. P.; Lang, G.; Lee, Y. J.; Scheidt, W. R.; Shelly, K.; Reed, C. A. *Inorg. Chem.* **1987**, *26*, 3022.
- (37) Masuda, H.; Taga, T.; Osaki, K.; Sugimoto, H.; Yoshida, Z.-I.; Ogoshi, H. *Inorg. Chem.* **1980**, *19*, 950.
- (38) Gonzales, J. A.; Wilson, L. J. *Inorg. Chem.* **1994**, *33*, 1543.
- (39) Gismelseed, A.; Bominaar, E. L.; Bill, E.; Trautwein, A. X.; Winkler, H.; Nasri, H.; Doppelt, P.; Mandon, D.; Fischer, J.; Weiss, R. *Inorg. Chem.* **1990**, *29*, 2741.
- (40) Simonato, J.-P.; Pécaut, J.; Le Pape, L.; Oddou, J.-L.; Jeandey, C.; Shang, M.; Scheidt, W. R.; Wojaczyński, J.; Wołowicz, S.; Latos-Grażyński, L.; Marchon, J.-C. *Inorg. Chem.* **2000**, *39*, 3978.
- (41) Fitzgerald, J. P.; Haggerty, B. S.; Rheingold, A. L.; May, L.; Brewer, G. A. *Inorg. Chem.* **1992**, *31*, 2006.
- (42) Palmer, S.; Stanton, J.; Jaggi, N.; Hoffman, B.; Ibers, S.; Schwartz, L. *Inorg. Chem.* **1985**, *24*, 2040.

The macrocycle is not planar as the diagram in Figure 2 shows. The core conformation is a rooflike folding where the bipyrrolic carbons are displaced with respect to the mean N<sub>4</sub> plane opposite the iron(III). The maximum deviation of the carbon atom from the N<sub>4</sub> plane equals 0.24 Å. The iron lies 0.583(1) Å out of the mean plane of the macrocycle and 0.502(5) Å out of the mean N<sub>4</sub> plane. However, these values are notably smaller when compared to two iron(III) porphycenes structurally characterized till now.<sup>12</sup> Namely, the relevant values equal for [(TPrPc)Fe<sup>III</sup>]<sub>2</sub>O 0.84 Å (the porphycene mean plane) and 0.67 Å (the N<sub>4</sub> mean plane) and for [(T(*t*-Bu)Pc)Fe<sup>III</sup>]<sub>2</sub>O 0.60 Å (the N<sub>4</sub> mean plane).<sup>12</sup> For these, displacements of high-spin five-coordinate iron from the porphyrin plane of 0.39–0.62 Å and from the N<sub>4</sub> plane of 0.39–0.54 Å are found.<sup>26–34</sup> The corresponding displacement values are typically smaller for the admixed spin state five-coordinate iron(III) porphyrins.<sup>24,35–39</sup>

In the solid, pairs of molecules are positioned about the center of symmetry so there is face-to-face  $\pi$ – $\pi$  contact. The two molecules do not fully overlay. Rather they are offset as is commonly seen when porphyrin macrocycles stack over one another. This offset is best seen by referring to Figure 3, which shows two views of the pair of molecules. The lower view is oriented so that one looks upon two nearly parallel planes.

Within this pair, the mean plane separation is 3.38 Å and the lateral shift of the porphycene center along the Fe–N bond is 4.49 Å. The distance from one porphycene center to the other is 5.602 Å, and the iron–iron separation is 6.304–(2) Å. The shortest C–C contact within this pair is 3.368 Å and involves C3–C9'. The lateral shift and the mean plane separation within [(TPrPc)Fe<sup>III</sup>Cl] place this molecule at the border region between I and W groups of the classification of Scheidt and Lee.<sup>29</sup> The I group contains the metalloporphyrin with an intermediate degree of  $\pi$ – $\pi$  overlap. The continuous decrease of  $\pi$ – $\pi$  overlap is characteristic for the W group.

It is interesting to note that the close C–C contact occurs also in the second pair. This is illustrated in Figure 3. The shortest C–C separation involves two *meso* carbons. Within this pair, the mean plane separation is 3.35 Å and the lateral shift of the porphycene centers along the iron and C9–C10 midpoint is 7.289 Å. The distance from one porphycene center to the other is 8.02 Å, and the iron–iron separation is 7.68 Å. The lateral shift and the mean plane separation within [(TPrPc)Fe<sup>III</sup>Cl] place this molecule in the W group of the classification of Scheidt and Lee. The Cl atom acts as an acceptor of two C(sp<sup>2</sup>)–H···Cl hydrogen bonds. Their geometric parameters (Table 2) suggest that these interactions are rather weak.<sup>43</sup>

**Crystal and Molecular Structure of (TPrPc)Fe<sup>II</sup>.** The structure of (TPrPc)Fe<sup>II</sup> has been determined by X-ray crystallography. The perspective view is shown in Figure 4.

A selection of important bond distances and angles are reported in Table 1. The iron atom is four-coordinate with

(43) Desiraju, G. R.; Steiner, T. *The Weak Hydrogen Bond in Structural Chemistry and Biology*; Oxford University Press: Oxford, 1999; pp 215–2221.

**Table 1.** Selected Bond Distances for Iron Porphycene Complexes

	(TPrPc)Fe <sup>II</sup> <sup>a</sup>	(TPrPc)Fe <sup>III</sup> Cl <sup>a</sup>	[(TPrPc)Fe <sup>III</sup> ] <sub>2</sub> O <sup>12</sup>	(OETAP)FeCl <sup>40</sup>	(PPIX)FeCl <sup>b</sup>	(Pc)FeCl <sup>41</sup>
Fe–N	1.932(5) 1.898(6)	2.000	2.052	1.929(7)	2.067(6)	1.945(4)
Fe–Cl		2.2508(9)		2.278(2)	2.218(6)	2.320(2)
N–Ct		1.929	0	1.897(3)	2.007(6)	1.871
Fe–N <sub>4</sub> displacement	0	0.510	0.67	0.352(3)	0.475(10)	0.30

<sup>a</sup> This work. <sup>b</sup> Koenig, D. F. *Acta Crystallogr.* **1965**, *18*, 663.

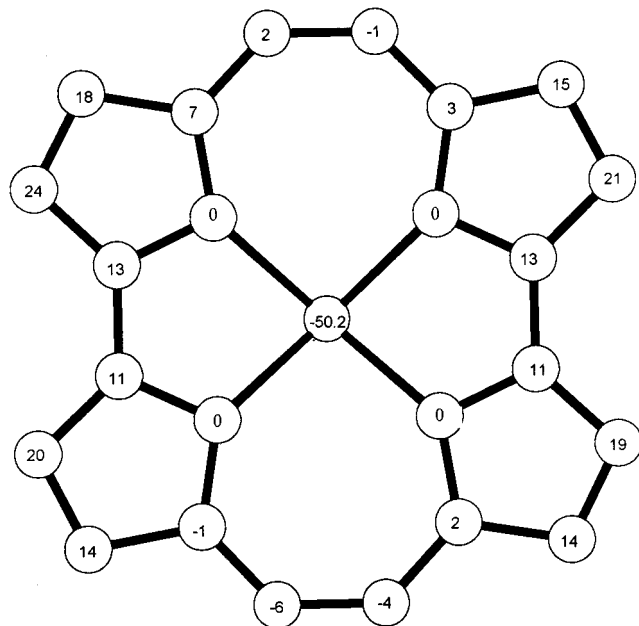


**Figure 2.** Diagram of the macrocyclic core of (TPrPc)Fe<sup>III</sup>Cl. Each atom symbol has been replaced by a number that represents the perpendicular displacement (in units of 0.01 Å) of from the mean porphyrine plane.

Fe–N bonds of nearly equal length (Fe–N in the range 1.988(6)–1.930(6) Å) to the four pyrrole nitrogen atoms. Thus, the bond lengths are similar to that found for nickel(II) porphyrine (1.90 Å).<sup>44</sup> The relatively short equatorial Fe–N bond distances are wholly consistent with the *S* = 1 intermediate-spin state of (TPrPc)Fe<sup>II</sup> with an unpopulated  $d_{x^2-y^2}$  orbital. Such an electronic structure has been previously identified on the basis of <sup>1</sup>H NMR spectra.<sup>20</sup> The Fe–N bond distances are slightly shorter than determined for the relevant four-coordinate intermediate-spin (*S* = 1) (OEP)Fe<sup>II</sup> (1.972 Å) and (TPP)Fe<sup>II</sup> (1.996 Å) compounds.<sup>45,46</sup> The macrocycle is planar. The iron lies in the mean plane of the macrocycle. In the solid, stacks of molecules are positioned along the *a* crystal axis so there is face-to-face  $\pi$ – $\pi$  contact. The molecules do not fully overlap. Rather they are offset as is commonly seen when porphyrin macrocycles stack over one another. Within the pair, the mean plane separation is 3.5 Å and the lateral shift of the porphyrine centers is 3.8 Å. The distance from one porphyrine center to the other is 5.196 Å. The lateral shift and the mean plane separation within [(TPrPc)Fe<sup>II</sup>] place this molecule in the I group of the classification of Scheidt and Lee.<sup>29</sup>

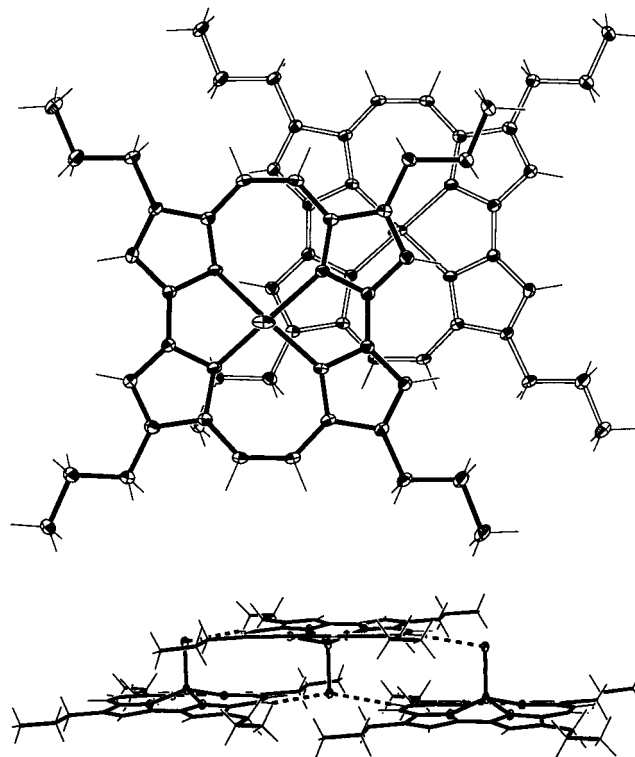


**Figure 3.** Views of a pair of (TPrPc)Fe<sup>III</sup>Cl molecules showing the overlap between adjacent molecules in the solid.

**Table 2.** Lengths (Å) and Angles (deg) of the Hydrogen Bonds

D–H···A <sup>a</sup>	D···A	H···A	D–H···A
C(10)–H(10)···Cl(1 <sup>i</sup> )	3.619 (3)	2.79	146
C(20)–H(20)···Cl(1 <sup>ii</sup> )	3.635 (3)	2.75	156

<sup>a</sup> Code of equivalent symmetry positions: (none) *x*, *y*, *z*; (i) 2 – *x*, 1 – *y*, –*z*; (ii) 1 – *x*, –*y*, –*z*.

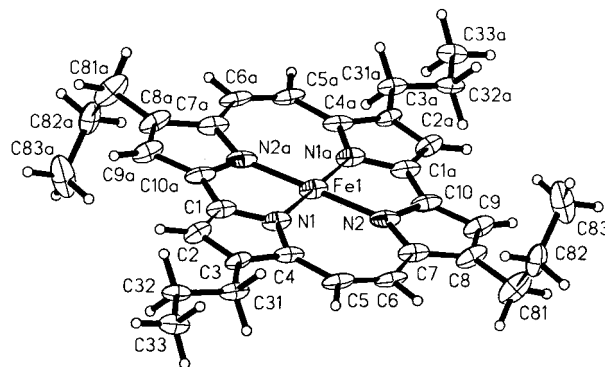


**Figure 4.** Perspective view of (TPrPc)Fe<sup>II</sup> showing 30% thermal contours.

Although the iron(II) porphyrine complex is not the main topic of this paper, we have found it essential to report its structural parameters to provide an adequate example of the iron porphyrine structure with an unpopulated  $d_{x^2-y^2}$  orbital.

(44) Vogel, E.; Balci, M.; Pramod, K.; Koch, P.; Lex, J.; Ermer, O. *Angew. Chem., Int. Ed. Engl.* **1987**, *26*, 928.

(45) Collman, J. P.; Hoard, J. L.; Kim, N.; Lang, G.; Reed, C. A. *J. Am. Chem. Soc.* **1975**, *97*, 2676.

(46) Strauss, S. H.; Silver, M. E.; Long, K. M.; Thomson, R. G.; Hudgens, R. A.; Spertalian, K.; Ibers, J. A. *J. Am. Chem. Soc.* **1985**, *107*, 4207.

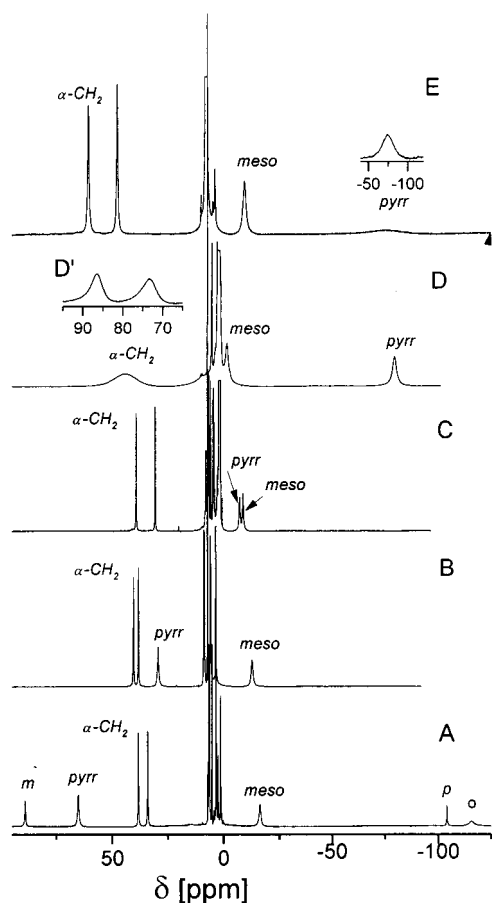


**Figure 5.**  $^1\text{H}$  NMR spectra of (A)  $(\text{TPrPc})\text{Fe}^{\text{III}}(\text{C}_6\text{H}_5\text{O})$ , (B)  $(\text{TPrPc})\text{Fe}^{\text{III}}\text{-Cl}$ , (C)  $(\text{TPrPc})\text{Fe}^{\text{III}}\text{-Br}$ , and (D)  $(\text{TPrPc})\text{Fe}^{\text{III}}(\text{ClO}_4)$ , all measured in dichloromethane- $d_2$  at 294 K. Inset D' shows the  $\alpha\text{-CH}_2$  region of the spectrum of  $(\text{TPrPc})\text{Fe}^{\text{III}}(\text{ClO}_4)$  at 203 K. Trace E presents the spectrum of  $(\text{TPrPc})\text{Fe}^{\text{III}}\text{-Cl}$  measured at 203 K in dichloromethane- $d_2$ . Labels: pyr, pyrrole H; meso, meso-H;  $\alpha\text{-CH}_2$ ,  $\alpha$ -methylene of the propyl substituent; o, m, and p, ortho H, meta H, and para H of the phenoxy ligand.

**$^1\text{H}$  NMR Studies of  $(\text{TPrPc})\text{Fe}^{\text{III}}\text{X}$ .** The  $^1\text{H}$  NMR spectra of  $(\text{TPrPc})\text{Fe}^{\text{III}}\text{X}$  are shown in Figure 5. The identity of the pyrrole resonances in these and all other spectra has been confirmed by a specific deuteration of the pyrrole positions to yield  $(\text{TPrPc}\text{-}d_4)\text{Fe}^{\text{III}}\text{X}$ . The meso and alkyl resonances have been assigned by their chemical shifts, intensities, and relative line widths. The doublet, detected for  $\alpha\text{-CH}_2$  protons of *n*-propyl groups, allowed an unambiguous identification of the five-coordinate structure for  $(\text{TPrPc})\text{Fe}^{\text{III}}\text{X}$  (where  $\text{X} = \text{PhO}^-$ ,  $\text{Cl}^-$ ,  $\text{Br}^-$ ,  $\text{I}^-$ ,  $\text{ClO}_4^-$ ) in dichloromethane- $d_2$  (Figure 5 and Table 3) and in other solvents used (Table 4).

Such a pattern results from a diastereotopic effect. The situation is more complex for  $(\text{TPrPc})\text{Fe}^{\text{III}}\text{ClO}_4$ , where the fast inversion of iron(III) with respect to the porphycene plane accounts for a broad singlet of  $\alpha\text{-CH}_2$  at 294 K in  $\text{CD}_2\text{Cl}_2$  (Figure 5, trace D) and in all other solvents used with the exception of  $\text{CDCl}_3$  (Table 4). However, in the slow exchange limit (203 K), a well-defined doublet has been detected (Figure 5, inset D'). Remarkably, the sign of the paramagnetic shift of the  $(\text{TPrPc})\text{Fe}^{\text{III}}\text{X}$  pyrrole resonances is determined by the choice of an axial ligand. Thus, downfield shifts have been determined for  $(\text{TPrPc})\text{Fe}^{\text{III}}\text{-Cl}$  ( $\text{C}_6\text{H}_5\text{O}$ ) and  $(\text{TPrPc})\text{Fe}^{\text{III}}\text{-Cl}$ , but large upfield ones have been

**Table 3.**  $^1\text{H}$  NMR Data for  $(\text{TPrPc})\text{Fe}^{\text{III}}\text{X}$  Complexes in Dichloromethane- $d_2$ <sup>a</sup>

compound	pyrr		meso		$\alpha\text{-CH}$	
	294 K	203 K	294 K	203 K	294 K	203 K
$(\text{TPrPc})\text{Fe}^{\text{III}}(\text{PhO})$	65.3	95.1	-13.3	-24.1	38.3	55.9
$(\text{TPrPc})\text{Fe}^{\text{III}}\text{-Cl}$	28.5	-73.4	-15.3	-11.9	34.1	50.8
$(\text{TPrPc})\text{Fe}^{\text{III}}\text{-Br}$	-7.8	-123.1	-9.3	-10.0	37.2	43.9
$(\text{TPrPc})\text{Fe}^{\text{III}}\text{-I}$	-49.4	-127.9	-0.4	-6.8	30.4	60.7
$(\text{TPrPc})\text{Fe}^{\text{III}}(\text{ClO}_4)$	-77.1	-123.3	-1.4	-7.5	25.4	71.0
					44 (br)	86.6
						73.2

<sup>a</sup> All chemical shifts relative to that of TMS.

detected for  $(\text{TPrPc})\text{Fe}^{\text{III}}\text{-Br}$ ,  $(\text{TPrPc})\text{Fe}^{\text{III}}\text{-I}$ , and  $(\text{TPrPc})\text{Fe}^{\text{III}}\text{-ClO}_4$  (294 K,  $\text{CD}_2\text{Cl}_2$ ). The  $\beta\text{-H}$  pyrrole chemical shifts span the remarkable +70 to -80 ppm range. The upfield relocation increases in the series  $\text{C}_6\text{H}_5\text{O}^-$ ,  $\text{Cl}^-$ ,  $\text{Br}^-$ ,  $\text{I}^-$ , and  $\text{ClO}_4^-$  at 294 K in dichloromethane- $d_2$ . The  $\beta\text{-H}$  pyrrole chemical shift of  $(\text{TPrPc})\text{Fe}^{\text{III}}(\text{C}_6\text{H}_5\text{O})$  (65.3 ppm), although of the same sign, is smaller than the  $\beta\text{-H}$  pyrrole shifts found in a group of high-spin  $(\text{TPP})\text{FeX}$  complexes ( $\text{X} = \text{C}_6\text{H}_5\text{O}^-$ ,  $\text{Cl}^-$ ,  $\text{Br}^-$ ,  $\text{I}^-$ ) where such a value is practically independent of the ligand and equals 80 ppm (293 K).<sup>21,22,47-49</sup> For instance, the dissimilarity is clearly pronounced for the chloro derivatives  $(\text{TPP})\text{Fe}^{\text{III}}\text{-Cl}$  (80 ppm) and  $(\text{TPrPc})\text{Fe}^{\text{III}}\text{-Cl}$  (28.5 ppm).

The variable-temperature  $^1\text{H}$  NMR spectra of  $(\text{TPrPc})\text{Fe}^{\text{III}}\text{-Cl}$  demonstrate an anti-Curie behavior (Figure 5, traces B and E). Particularly the downfield shift of the  $\beta\text{-H}$  pyrrole resonance (294 K) is transformed into an upfield shift at the low-temperature range assuming a 0 ppm value of the paramagnetic shift at ca. 250 K. The relevant plots of pyrrole chemical shifts as a function of the inverse temperature are shown in Figure 6. (The complete plots are included in the Supporting Information.)

The behavior of the isotropic shift is specific for each complex. Typically the  $1/T$  dependence is nonlinear. An attempt of a linear extrapolation with respect to  $1/T$  on the basis of observed shifts at the lower temperature limit (233–193 K) resulted in unrealistic intercepts far from the diamagnetic position. The apparent intercepts of the imposed straight line for  $(\text{TPrPc})\text{Fe}^{\text{III}}(\text{C}_6\text{H}_5\text{O})$ ,  $(\text{TPrPc})\text{Fe}^{\text{III}}\text{-Cl}$ ,  $(\text{TPrPc})\text{Fe}^{\text{III}}\text{-Br}$ ,  $(\text{TPrPc})\text{Fe}^{\text{III}}\text{-I}$ ,  $(\text{TPrPc})\text{Fe}^{\text{III}}(\text{ClO}_4)$  are -1.3, 433.0, 197.0, 116.0, and 28.0 ppm, respectively.

$^1\text{H}$  NMR spectroscopy of paramagnetic iron porphyrins provides a particularly useful tool for characterizing the oxidation/spin/ligation states of the iron.<sup>21,22</sup> Recently we have shown that in the series of iron porphycene derivatives  $(\text{TPrPc})\text{Fe}^{\text{II}}$ ,  $(\text{TPrPc})\text{Fe}^{\text{III}}\text{-O-Fe}^{\text{III}}(\text{TPrPc})$ ,  $(\text{TPrPc})\text{Fe}^{\text{III}}\text{-O-O-Fe}^{\text{III}}(\text{TPrPc})$ , and  $\text{B}(\text{TPrPc})\text{Fe}^{\text{IV}}\text{O}$  the positions of the  $\beta\text{-H}$  pyrrole resonances resemble those found for the correspond-

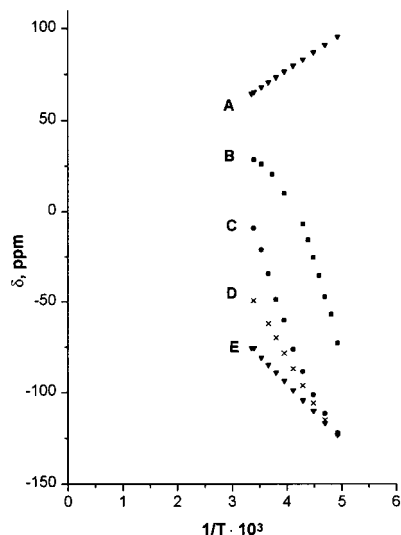
(47) La Mar, G. N.; Eaton, G. R.; Holm, R. H.; Walker, F. A. *J. Am. Chem. Soc.* **1973**, *95*, 63.

(48) La Mar, G.; Walker, F. A. Nuclear Magnetic Resonance of Paramagnetic Metalloporphyrins. In *The Porphyrins*; Dolphin, E., Ed.; Academic Press: New York, 1979; Vol. IVB, pp 57–161.

(49) Wojaczyński, J.; Latos-Grażyński, L.; Hrycyk, W.; Pacholska, E.; Rachlewicz, K.; Szyrenberg, L. *Inorg. Chem.* **1996**, *35*, 6861.

**Table 4.** Solvent Dependence of the Chemical Shifts of the  $\beta$ -Pyrrole and  $\alpha$ -CH<sub>2</sub> <sup>1</sup>H NMR Resonances for (TPrPc)Fe<sup>III</sup>X Complexes<sup>a</sup>

compound	dichloromethane- <i>d</i> <sub>2</sub>		chloroform- <i>d</i>		acetonitril- <i>d</i> <sub>3</sub>		acetone- <i>d</i> <sub>6</sub>		benzene- <i>d</i> <sub>6</sub>		toluene- <i>d</i> <sub>8</sub>	
	$\beta$ -pyrr	$\alpha$ -CH <sub>2</sub>	$\beta$ -pyrr	$\alpha$ -CH <sub>2</sub>	$\beta$ -pyrr	$\alpha$ -CH <sub>2</sub>	$\beta$ -pyrr	$\alpha$ -CH <sub>2</sub>	$\beta$ -pyrr	$\alpha$ -CH <sub>2</sub>	$\beta$ -pyrr	$\alpha$ -CH <sub>2</sub>
(TPrPc)Fe(PhO)	64.4	38.3	64.9	38.0			66.5	38.2	66.2	36.9	66.7	36.7
		34.1		34.1	insoluble			33.5		31.5		31.6
(TPrPc)FeCl	28.5	39.3	26.8	38.7	25.6	40.0	46.0	40.0	52.3	40.7	59.9	40.4
		37.2		36.3		36.2		38.9		36.6		36.5
(TPrPc)FeBr	-7.8	39.0	-4.6	38.1			17.0	39.7	32.6	38.0 <sup>b</sup>	36.7	38.6
		30.4		30.5	insoluble			35.0				38.0
(TPrPc)FeI	-49.4	40.5	-51.0	35.7	-66.3	40.0 <sup>b</sup>	-36.0	39.2	-23.7	38.6	-19.6	36.1
		25.4		21.2		30.0 <sup>b</sup>		25.4		29.4		31.4
(TPrPc)Fe(ClO <sub>4</sub> )	-76.9	44.5 <sup>b</sup>	-75.2	47.4 <sup>b</sup>	-78.2	46.5 <sup>b</sup>	-71.1	39.2 <sup>b</sup>	-75.8	54.6 <sup>b</sup>	-75.7	41.4 <sup>b</sup>
				30.5 <sup>b</sup>								

<sup>a</sup> 294 K. <sup>b</sup> Broad.**Figure 6.** Pyrrole chemical shift versus  $1/T$  for (A) (TPrPc)Fe<sup>III</sup>(C<sub>6</sub>H<sub>5</sub>O), (B) (TPrPc)Fe<sup>III</sup>Cl, (C) (TPrPc)Fe<sup>III</sup>Br, (D) (TPrPc)Fe<sup>III</sup>I, and (E) (TPrPc)Fe<sup>III</sup>(ClO<sub>4</sub>).

ing iron porphyrin derivatives as far as a general pattern is concerned.<sup>20</sup> The  $\alpha$ -CH<sub>2</sub> resonances of the propyl groups follow the pattern, but they are downfield shifted practically in each considered case. Thus, only their relative values of the paramagnetic shift might be helpful in the spectroscopic analysis.

The contact shifts are indicative of which iron d orbital and porphyrin molecular orbital are involved in the transmission of the unpaired electron in the macrocycle periphery.<sup>21,22</sup> The analogous correlation is expected to be valid for iron porphycenes as well. Generally the ground state of the iron(III) porphycene can be related to the following models of the electronic configuration:

(i) low spin  $(d_{xy})^2(d_{xz}d_{yz})^3(d_z)^0(d_{x^2-y^2})^0$  or  $(d_{xz}d_{yz})^4(d_{xy})^1(d_z)^0(d_{x^2-y^2})^0$ ,

(ii) high spin  $(d_{xy})^1(d_{xz})^1(d_{yz})^1(d_z)^1(d_{x^2-y^2})^1$ ,

(iii) intermediate spin  $(d_{xy})^2(d_{xz})^1(d_{yz})^1(d_z)^1(d_{x^2-y^2})^0$ .

These configurations should be clearly distinguishable by <sup>1</sup>H NMR spectroscopy. In the regular low-spin case one can expect the upfield position of the pyrrole resonances due to the transmission of the spin density from  $(d_{xz}d_{yz})^3$  to the  $\pi$  filled orbitals of porphycene. In the less common low-spin case the pyrrole H resonance should be shifted very little because of localization of the unpaired electron on the  $d_{xy}$  orbital of iron(III), which, because of its symmetry, overlaps

to a smaller extent with the  $\pi$  orbitals of porphycene. In the case of the high-spin iron(III) center both  $\sigma$  and  $\pi$  delocalization routes can operate, resulting in downfield  $\beta$ -H shifts.<sup>21,22,47-49</sup>

The intermediate  $S = 3/2$  ground electronic state should be characterized by an upfield shift as the low-spin one as the identical delocalization path is operating. The shift value is expected to be large as there are two  $\pi$  symmetry unpaired electrons in the  $S = 3/2$  state in comparison to that for  $S = 1/2$ .<sup>21,22,40,50-56</sup>

In several cases the pure  $S = 5/2$  and pure  $S = 3/2$  electronic states are closely spaced so the spin-orbit coupling provides the mechanism for mixing them.<sup>24,37,57-61</sup> <sup>1</sup>H NMR spectra are quite sensitive to the  $S = 5/2$  and  $S = 3/2$  contributions in the spin-admixed complexes.<sup>25,54,55,61-63</sup> In addition temperature changes affect the contribution of the two states with a dramatic effect on the pyrrole proton shifts.<sup>25,32-34,58-60,64</sup> However, the thermal equilibrium between two pure spin states may result in identical <sup>1</sup>H NMR behavior. Consequently it may be difficult to discriminate between spin equilibria and spin-admixed states solely on the basis of <sup>1</sup>H NMR investigations.<sup>25</sup>

Several examples of pure  $S = 3/2$  iron(III) porphyrins have been reported presenting typically a strong upfield shift for  $\beta$ -H.<sup>25,54,55</sup> Strong upfield chemical shifts have been detected for (2,4,6-(OMe)<sub>3</sub>TPP)Fe<sup>III</sup>ClO<sub>4</sub> (-30.6 ppm) (CDCl<sub>3</sub>, 298 K)<sup>24,63</sup> and iron(III) porphyrin with vinyl carbene inserted

- (50) Latos-Grażyński, L.; Cheng, R.-J.; La Mar, G. N.; Balch, A. L. *J. Am. Chem. Soc.* **1981**, *103*, 4270.
- (51) Mansuy, D.; Morgenstern-Baderau, I.; Lange, M.; Gans, P. *Inorg. Chem.* **1982**, *21*, 1427.
- (52) Balch, A. L.; Cheng, R.-J.; La Mar, G. N.; Latos-Grażyński, L. *Inorg. Chem.* **1985**, *24*, 2651.
- (53) Artaud, I.; Gregoire, N.; Leduc, P.; Mansuy, D. *J. Am. Chem. Soc.* **1990**, *112*, 6899.
- (54) Reed, C. A.; Guiset, F. *J. Am. Chem. Soc.* **1996**, *118*, 3281.
- (55) Evans, D. R.; Reed, C. A. *J. Am. Chem. Soc.* **2000**, *122*, 4660.
- (56) Ikeue, T.; Saitoh, T.; Yamaguchi, T.; Ohgo, Y.; Nakamura, M.; Takahashi, M.; Takeda, M. *Chem. Commun.* **2000**, 1989.
- (57) Dolphin, D. H.; Sams, J. R.; Tsin, T. B. *Inorg. Chem.* **1977**, *16*, 711.
- (58) Maltempo, M. M. *J. Chem. Phys.* **1974**, *61*, 2540.
- (59) Maltempo, M. M.; Moss, T. H.; Cusanovich, M. A. *Biochim. Biophys. Acta* **1974**, *342*, 290.
- (60) Maltempo, M. M.; Moss, T. H. *Q. Rev. Biophys.* **1976**, *9*, 181.
- (61) Goff, H. M.; Shimomura, E. *J. Am. Chem. Soc.* **1980**, *102*, 31.
- (62) Boersma, A. D.; Goff, H. M. *Inorg. Chem.* **1982**, *21*, 581.
- (63) Goff, H. M., M. Nuclear Magnetic Resonance of Iron Porphyrins. In *Iron Porphyrins Part I*; Lever, A. B. P., Gray, H., Eds.; Addison-Wesley: Reading, MA, 1983; p 237.
- (64) Toney, G. E.; terHaar, L. W.; Savrin, J. E.; Gold, A.; Hatfield, W. E.; Sangaiah, R. *Inorg. Chem.* **1984**, *23*, 2563.

between iron and the pyrrole nitrogen (25.7, -19.7, -23.9, and -40.5 ppm) (298 K, CDCl<sub>3</sub>),<sup>52</sup> with the most upfield value determined for (TPP)Fe<sup>III</sup>(CB<sub>11</sub>H<sub>6</sub>Br<sub>6</sub>) (-62 ppm) (C<sub>6</sub>D<sub>6</sub>, 298 K).<sup>55</sup>

Thus, the contact shift pattern of (TPrPc)Fe<sup>III</sup>X measured at 203 K of Table 3 reflects extensive spin delocalization into the  $\pi$  molecular orbital of porphycene similarly to that found for iron(III) porphyrin complexes. The dominance of the  $\pi$  spin transfer mechanism can also be taken as direct evidence that  $d_{x^2-y^2}$  is weakly populated or not populated at this temperature. The <sup>1</sup>H NMR spectrum of low-spin [(TPrPc)Fe<sup>III</sup>(Im)<sub>2</sub>]<sup>+</sup> measured at 223 K reveals that the paramagnetic shift of the  $\beta$ -H resonance equals -19.7, clearly pointing out the difference in the extent of  $\pi$  delocalization, which is smaller for the  $S = 1/2$  ground electronic state in comparison to  $S = 3/2$  as rationalized above. The intermediate-spin iron(II) porphycene also demonstrated a strongly upfield shifted pyrrole resonance (-37.52 ppm) at 293 K accounted for by depopulation of the  $d_{x^2-y^2}$  orbital in the  $(d_{xy})^2(d_{xz})^2(d_{yz})^1(d_{x^2-y^2})^0$  electronic structure.<sup>20</sup>

Considering the values of the chemical shifts and pronounced non-Curie behavior of the pyrrole as well as *meso* signals demonstrated in the variable-temperature experiments, one can conclude that the (TPrPc)Fe<sup>III</sup>Cl, (TPrPc)Fe<sup>III</sup>Br, and (TPrPc)Fe<sup>III</sup>I complexes reveal the admixed  $S = 3/2$ ,  $5/2$  ground electronic state, with a dominating contribution of the  $S = 3/2$  one. Once temperature increases the  $S = 5/2$  contribution gains importance as clearly illustrated by the positive deviation from the Curie law for all pyrrole resonances and the values of the intercepts found for the forced linear extrapolations.

In terms of the chemical shift (TPrPc)Fe<sup>III</sup>(ClO<sub>4</sub>) and recently reported [(TPrPc)Fe<sup>III</sup>(THF)<sub>2</sub>](ClO<sub>4</sub>)<sup>17</sup> can be considered as examples of the purest  $S = 3/2$  state in the series where the corresponding shift sets the limits at any temperature considered. The high-spin limit behavior is exemplified, at least at 294 K, by (TPrPc)Fe<sup>III</sup>(C<sub>6</sub>H<sub>5</sub>O). Apart from the distinctive downfield pyrrole resonance position, we have identified axial ligand resonances at (ortho) -115.47 ppm, (meta) 89.16 ppm, and (para) -104.18 ppm (294 K, CD<sub>2</sub>-Cl<sub>2</sub>). The resonance assignments for this ligand are based on the previous assignments of phenoxy complexes, intensities of the resonances, and line widths.<sup>65-67</sup> These values are slightly smaller when compared to those found for (TTP)-Fe<sup>III</sup>(C<sub>6</sub>H<sub>5</sub>O): ortho, -118.4 ppm; meta, 95 ppm; para, -109.7 ppm (298 K, C<sub>7</sub>D<sub>8</sub>).<sup>67</sup> The detected differences reflect some contribution of the  $S = 3/2$  state in the ground electronic state of (TPrPc)Fe<sup>III</sup>(C<sub>6</sub>H<sub>5</sub>O). As determined for the corresponding aryloxy iron(III) porphyrin complexes, the opposite signs of the shifts for meta versus ortho and para protons are indicative of  $\pi$  spin density on the aryloxy ligand and require that the iron(III)  $d_{x^2-y^2}$  orbital is half-occupied.<sup>65-67</sup>

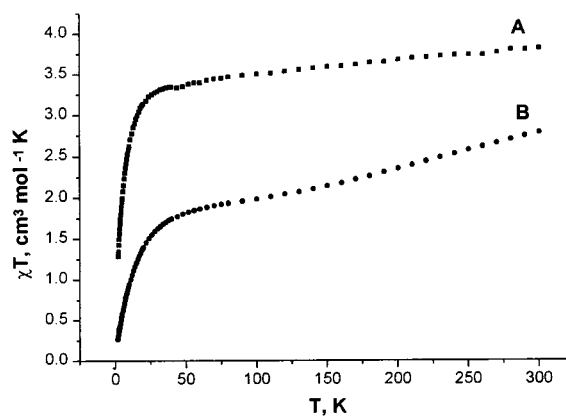


**Figure 7.** Temperature dependence of the  $\chi_M T$  product for microcrystalline samples of (TPrPc)Fe<sup>III</sup>Cl (A) and (TPrPc)Fe<sup>III</sup>Br (B) in the range 2–300 K.

The most upfield position of the *meso*-H resonance (Table 3) is observed for (TPrPc)Fe<sup>III</sup>(C<sub>6</sub>H<sub>5</sub>O), with the largest  $S = 5/2$  contribution in the series. (TPrPc)Fe<sup>III</sup>(ClO<sub>4</sub>) demonstrates a less upfield shifted *meso*-H position than any compound in the group. This observation leads to the conclusion that the  $S = 5/2$  state locates more of the positive spin density at the *meso* position than the  $S = 3/2$  one does.

**Magnetization Measurements.** The magnetization properties of microcrystalline samples of (TPrPc)Fe<sup>III</sup>Cl and (TPrPc)Fe<sup>III</sup>Br have been investigated to evaluate the spin state of the iron centers. Figure 7 illustrates the temperature dependence of the product of molar susceptibility and temperature.

The Curie–Weiss plot of (TPrPc)Fe<sup>III</sup>Cl is not strictly linear. The plot of  $\chi_M T$  demonstrates that this value varies in the relatively small range 3.4–3.8 cm<sup>3</sup> K mol<sup>-1</sup> ( $\mu_{\text{eff}} = 5.2$ – $5.5 \mu_B$ ) at the 50–300 K limits. These values are too low for high-spin iron(III) (4.37 cm<sup>3</sup> K mol<sup>-1</sup> or  $5.9 \mu_B$ ) and too high for the intermediate-spin (1.87 cm<sup>3</sup> K mol<sup>-1</sup> or  $3.9 \mu_B$ ) assignment. At lower temperatures the  $\chi_M T$  product decreases to 1.32 cm<sup>3</sup> K mol<sup>-1</sup> ( $3.25 \mu_B$ ) at 2.1 K. Such a behavior of magnetic susceptibility might be expected in the framework of the admixed  $S = 3/2$ ,  $5/2$  spin model, with a dominating  $S = 5/2$  contribution, presuming that the complex presents a zero-field splitting component to account for the low-temperature limit.<sup>39</sup> The possibility of a spin–spin interaction can be instrumental as well since the minimum distances between adjacent paramagnetic centers are relatively small. The crystal structure of (TPrPc)Fe<sup>III</sup>Cl shows the arrangement of the molecules in double layers with opposite orientation of the Fe–Cl bonds in the neighboring layers and a very short interlayer distance of 3.38 Å (Figure 2). On this basis, the reason for the magnetic properties can be related to interactions between oppositely oriented molecules inside the double layers. However, a detailed analysis of the ground electronic state has not been carried out. The microcrystalline samples obtained in the bulk syntheses may be polymorphic, and they may contain a mixture of structurally similar species<sup>38</sup> or reveal different effects of solvation.<sup>54,55</sup> Thus, examination of (TPrPc)Fe<sup>III</sup>X with bulk physical probes such as magnetic susceptibility affords a resultant measurement for the different species

(65) Goff, H. M.; Shimomura, E. T.; Lee, Y. J.; Scheidt, W. R. *Inorg. Chem.* **1984**, *23*, 315.

(66) Pyrz, J. W.; Roe, A. L.; Stern, L. J.; Que, L., Jr. *J. Am. Chem. Soc.* **1985**, *107*, 614.

(67) Arasasingham, R. D.; Balch, A. L.; Hart, R.; Latos-Grażyński L. *J. Am. Chem. Soc.* **1990**, *112*, 7566.

which may be present in the samples. Actually the existence of two crystallographically distinct orientations of the disordered (TPrPc)Fe<sup>III</sup>Cl molecules has been determined by X-ray crystallography. Preliminary Mössbauer data reveal the presence of high-spin and admixed spin components.<sup>68</sup>

Remarkably the plot of the reciprocal magnetic susceptibility for (TPrPc)Fe<sup>III</sup>Br demonstrates strong deviation from linearity, with a well-defined inflection at ca. 100 K. The temperature dependence of the product of molar susceptibility and temperature is shown in Figure 7. The value of the  $\chi_M T$  product decreased smoothly from 2.87 cm<sup>3</sup> K mol<sup>-1</sup> ( $\mu_{\text{eff}} = 4.7 \mu_B$ ) at 298 K to 1.83 cm<sup>3</sup> K mol<sup>-1</sup> ( $\mu_{\text{eff}} = 3.9 \mu_B$ ) at 50 K. Such a behavior can be related to the quantum-mechanical admixed  $S = 3/2, 5/2$  spin state.<sup>39</sup> At the 50–4 K limits the  $\chi_M T$  product decreases below the 1.87 cm<sup>3</sup> K mol<sup>-1</sup> pure spin value to approach 0.45 cm<sup>3</sup> K mol<sup>-1</sup> at 4 K. A decrease of the value of the  $\chi_M T$  product can be expected if the ground electronic state of the complex presents a zero-field splitting component.<sup>40,69,70</sup> At the very low-temperature limit we have found a behavior deviating from the Curie–Weiss law, indicating possible antiferromagnetic interactions resembling those detected for (TPP)Fe<sup>III</sup>(B<sub>11</sub>CH<sub>12</sub>).<sup>36</sup>

## Discussion

In general the results of our investigations are all in accord with the admixed  $S = 3/2, 5/2$  ground electronic state in the series of five-coordinate iron(III) porphycene complexes.

The admixed  $S = 3/2, 5/2$  state, investigated in detail for five- and six-coordinate iron(III) porphyrins and five-coordinate iron(III) phthalocyanines and iron(III) tetraazaporphyrin, demonstrates magnetic properties that are distinctively contained in the range between the limits of the pure  $S = 3/2$  and  $S = 5/2$  states. These include magnetic moments between 3.9 and 5.9  $\mu_B$  and EPR  $g_i^{\text{eff}}$  values between 4 and 6.<sup>21,22,54,55,70–72</sup> Mössbauer quadrupole splitting values are contained in the 3–4.2 mm/s range for the  $S = 3/2$  state, and this value decreases with increasing  $S = 5/2$  character in the spin-admixed state.<sup>54,68,57,73</sup> The  $\beta$ -H pyrrole shift values of (TPP)Fe<sup>III</sup>X shift dramatically upfield with increasing  $S = 3/2$  character.<sup>21,22,54,55,61–63</sup> Evidently, the

corresponding physicochemical parameters determined for (TPrPc)Fe<sup>III</sup>X ( $X = C_6H_5O^-, Cl^-, Br^-, I^-, ClO_4^-$ ) fit the admixed ground electronic state characteristics.

The theoretical analysis based on crystal field theory indicates that increasing tetragonal distortion in ferric tetraphenylporphyrin (e.g., decreasing axial field strength) will eventually stabilize the intermediate-spin state ( $S = 3/2$ ) when the  $d_z^2$  orbital is close in energy to the  $d_{xy}, d_{xz},$  and  $d_{yz}$  orbitals and singly occupied, and the  $d_{x^2-y^2}$  is considerably higher in energy and vacant.<sup>58–60,74</sup> A preference between high- and intermediate-spin states depends also on the energy separation between the  $d_{x^2-y^2}$  and  $d_{xy}$  orbitals. It provides another potential instrument for stabilizing the pure intermediate-spin state ( $S = 3/2$ ) via an increase of the  $d_{x^2-y^2}$  orbital energy, which is controlled by the field strength of the equatorial ligand. Consequently the mixed-spin and nearly pure intermediate-spin states found for the chloroiron(III) complexes of phthalocyanine<sup>42</sup> and tetraazaporphyrin,<sup>41</sup> respectively, are related to the stronger interaction of these macrocycles with the iron  $d_{x^2-y^2}$  orbital, due to their smaller hole relative to that of the porphyrins. Thus, the combination of a weak axial field and a small tetramethylchirophyrin porphyrin ((TMCP)H<sub>2</sub>) hole in the [(TMCP)Fe<sup>III</sup>(C<sub>2</sub>H<sub>5</sub>OH)<sub>2</sub>]<sup>+</sup> and [(TMCP)Fe<sup>III</sup>(C<sub>2</sub>H<sub>5</sub>OH)(H<sub>2</sub>O)]<sup>+</sup> species resulted in a ground state which is an intermediate-spin or nearly intermediate-spin state ( $S = 3/2$ ).<sup>40</sup>

The present investigation emphasizes the resemblance and fundamental differences between iron porphycenes and iron porphyrins observed at the five-coordinate iron(III) level. Using the strength of the equatorial ligand as the criterion, one can place porphycene on the borderline between porphyrins and tetraazaporphyrins,<sup>41</sup> i.e., in the position adjacent to phthalocyanines.<sup>42</sup>

The rather simple picture for the (TPrPc)Fe<sup>III</sup>X group detected in dichloromethane-*d*<sub>2</sub> solutions by <sup>1</sup>H NMR is more complex in the solid state. One has to notice that the delicate balance typical for the admixed spin state is controlled apart from the nature of the axial and equatorial contributions and by external factors. This opinion is clearly supported by the observation of a strong solvent effect in the <sup>1</sup>H NMR spectra of (TPrPc)Fe<sup>III</sup>X (Table 4). The replacement of the solvent typically used in our <sup>1</sup>H NMR investigations, i.e., dichloromethane-*d*<sub>2</sub> by toluene-*d*<sub>8</sub>, causes a marked increase of the  $S = 5/2$  character in the admixed ground electronic state as demonstrated by a downfield relocation of the pyrrole resonances including the spectacular change of the sign of the isotropic shift seen for (TPrPc)Fe<sup>III</sup>Br (Table 4). Thus, a solid-state effect such as intermolecular coupling, effect of solvation, etc. may considerably change the electronic structure compared to these detected in solution. The solid-state or frozen-solution data presented in this paper are generally consistent with the presence of the admixed ground electronic spin state. In the case of (TPrPc)Fe<sup>III</sup>Cl the admixed spin form is accompanied by a high-spin state as found by Mössbauer<sup>68</sup> and EPR<sup>75</sup> spectroscopy. The decrease of the  $\chi_M T$  product for (TPrPc)Fe<sup>III</sup>Cl and (TPrPc)Fe<sup>III</sup>Br

(68) Preliminary Mössbauer data collected for the (TPrPc)Fe<sup>III</sup>Cl complex presented a rather complex picture. The spectrum measured at 293 K consists of two doublets [(A)  $\Delta E_q = 0.0, \delta = 0.33$ ; (B)  $\Delta E_q = 1.50, \delta = 0.23$  (mm s<sup>-1</sup>)]. The temperature decrease to 10 K preserves the number of species although the spectroscopic parameters change markedly [(A)  $\Delta E_q = 1.03, \delta = 0.32$ ; (B)  $\Delta E_q = 2.83, \delta = 0.26$  (mm s<sup>-1</sup>)]. The first set of parameters has been assigned to the admixed electronic state form and the second to the high-spin component. The  $\Delta E_q$  value of the admixed form increased from 1.50 to 2.83 mm s<sup>-1</sup> once the temperature was lowered from 293 to 10 K as expected for such an electronic structure.<sup>39,69</sup>

(69) Keutel, H.; Käpplinger, I.; Jäger, E.-G.; Grodzicki, M.; Schünemann, V.; Trautwein, A. X. *Inorg. Chem.* **1999**, *38*, 2320.

(70) Mitra, S. Magnetic Susceptibility of Iron Porphyrins. In *Iron Porphyrins Part II*; Lever, A. B. P., Gray, H., Eds.; Addison-Wesley: Reading, MA, 1983; p 1.

(71) Palmer, G. Electron Paramagnetic Resonance of Hemoproteins. In *Iron Porphyrins Part II*; Lever, A. B. P., Gray, H., Eds.; Addison-Wesley: Reading, MA, 1983; p 43.

(72) Bominaar, E. L.; Ding, X.-Q.; Gismelseed, A.; Bill, E.; Winkler, H.; Trautwein, A. X.; Nasri, H.; Fischer, J.; Weiss, R. *Inorg. Chem.* **1992**, *31*, 1845.

(73) Kostka, K. L.; Fox, B. G.; Hendrich, M. P.; Collins, T. J.; Rickard, C. E. F.; Wright, L. J.; Münck, E. *J. Am. Chem. Soc.* **1993**, *115*, 6746.

(74) Boominaar, E. L.; Block R. *J. Chem. Phys.* **1991**, *95*, 6712.



derivatives in the 300–50 K temperature limits indicates the decreasing  $S = 5/2$  contribution once the temperature has been decreasing. Consequently the X-ray data of (TPrPc)-Fe<sup>III</sup>Cl measured at 110 K can be considered as characteristic for the admixed electronic structure of iron(III) porphycene.

Significantly the extent of the  $S = 5/2$  contribution in the admixed  $S = 3/2, 5/2$  ground electronic state, as gradated solely on the basis of the pyrrole proton paramagnetic shifts, is controlled by the strength of the axial ligand and increases in the series  $\text{ClO}_4^- < \text{I}^- < \text{Br}^- < \text{Cl}^- < \text{C}_6\text{H}_5\text{O}^-$ . This order reflects the basic features of the magnetochemical series introduced by Reed and co-workers.<sup>54,55,76</sup> Elements of this idea were noted much earlier by Reed<sup>24</sup> and Goff.<sup>62,63</sup>

Originally the method for ranking ligand field strength was based on the degree of  $S = 3/2, 5/2$  admixture caused by an axial ligand in five-coordinate iron(III) tetraphenylporphyrin, applying the paramagnetic shift of the  $\beta$ -H pyrrole resonance as a major criterion. Since stronger ligands, e.g.,  $\text{I}^-$ ,  $\text{Br}^-$ , and  $\text{Cl}^-$ , produced analogous high-spin iron(III) porphyrin complexes, the series could be extended only by changing the equatorial ligand (from porphyrin to phthalocyanine) and as a consequence resorting to other physicochemical probes. Thus, the magnetic moment, zero-field splitting, and quadrupole splitting were used as measured in the solid state, bearing, however, the burden of possible solid-state effects.<sup>54</sup> Finally the following series, represented here in its shorter form, has been determined:  $\text{SbF}_6^- < \text{H}_2\text{O} < \text{ClO}_4^- < \text{CF}_3\text{SO}_3^- < \text{BF}_4^- < \text{ReO}_4^- < \text{I}^- < \text{Br}^- < \text{OH}^- \approx \text{Cl}^- < \text{OAc}^- < \text{O}(\text{p-NO}_2) < \text{O}(\text{p-NO}_2) < \text{F}^- < \text{RS}^-$ .<sup>55</sup> The reversal of the  $\text{H}_2\text{O}$  and  $\text{OH}^-$  ligand field strengths on the magnetochemical series relative to the spectrochemical series has been discussed.<sup>55</sup> The magnetochemical series reflects the ligand field effect dominated by  $\sigma$ -bonding and electrostatic interactions.<sup>55</sup> Evans and Reed commented<sup>55</sup> that in the (TMCP)Fe<sup>III</sup>Br (84.6 ppm), (TMCP)Fe<sup>III</sup>Cl (90.7 ppm), and (TMCP)Fe<sup>III</sup>(OH) (91.9 ppm) groups ( $X = \text{Cl}^-$ ,  $\text{Br}^-$ ,  $\text{OH}^-$ ) the averaged pyrrole proton shifts (given in parentheses)<sup>55</sup> suggest the magnetic ordering  $\text{Br}^- < \text{Cl}^- \approx \text{OH}^-$ .<sup>55</sup> We have found it important to make the point that the recently reported [(TMCP)Fe<sup>III</sup>(C<sub>2</sub>H<sub>5</sub>OH)<sub>2</sub>]<sup>+</sup> (−30.7 ppm) and [(TMCP)Fe<sup>III</sup>(D<sub>2</sub>O)<sub>2</sub>]<sup>+</sup> (−35.0 ppm) complexes demonstrated averaged  $\beta$ -H pyrrole shifts (in parentheses) which follow the tetraarylporphyrin series.<sup>40</sup> In particular the reversal of the  $\text{H}_2\text{O}$  and  $\text{OH}^-$  ligand field strengths has been independently confirmed.

In terms of the magnetochemical series, the iron(III) 1,7-, 12,17-tetrapropylporphycene, soluble in typical organic solvents, can be considered as an alternative and universal framework to classify the ligand strength in a magnetochemical series, consistently using the  $\beta$ -H pyrrole paramagnetic shift as a fundamental criterion. It allows the whole

(75) The EPR spectra of (TPrPc)Fe<sup>III</sup>Cl (toluene, 7 K) are accounted for by two species. Effective  $g$  values of the first component ( $g_1 = 6.18$ ,  $g_2 = 5.80$ ,  $g_3 = 2.00$ ) are characteristic for an  $S = 5/2$  ground electronic state with zero-field splitting and a rhombic contribution to the ligand field. The second component ( $g_1 = 4.31$ ,  $g_2 = 4.17$ ,  $g_3 = 2.00$ ) reveals features typical for the admixed spin state with the domination of the  $S = 3/2$  contribution.<sup>23,24,38–40,55,60,63,69,71</sup>

(76) Reed, C. A. *Inorg. Chim. Acta* **1997**, 263, 95.

**Table 5.** Summary of Crystal Data for (TPrPc)Fe<sup>III</sup>Cl (**1**) and (TPrPc)Fe<sup>II</sup> (**2**)

	<b>1</b>	<b>2</b>
empirical formula	C <sub>32</sub> H <sub>36</sub> N <sub>4</sub> ClFe	C <sub>32</sub> H <sub>36</sub> N <sub>4</sub> Fe
mol wt	576.95	532.50
$T$ , K	100(2)	100(2)
$\lambda$ , Å	0.71073	0.71073
cryst syst	triclinic	triclinic
space group	<i>P1</i>	<i>P1</i>
$a$ , Å	9.496(2)	5.196(1)
$b$ , Å	12.281(2)	9.857(2)
$c$ , Å	13.338(3)	12.506(3)
$\alpha$ , deg	112.22(3)	81.17(3)
$\beta$ , deg	97.85(3)	84.85(2)
$\gamma$ , deg	96.76(3)	89.29(3)
$V$ , Å <sup>3</sup>	1401.9(5)	630.4(2)
$Z$	1	1
$D_c$ , Kg m <sup>−3</sup>	1.345	1.403
$F(000)$	598	282
$\mu(\text{Mo K}\alpha)$ , mm <sup>−1</sup>	0.661	0.628
no. of data	10413	4090
no. of unique data	6514	2674
no. of params	496	171
$R1^a$	0.0417	0.0875
$S$	1.069	0.95
wR2 <sup>a</sup>	0.0959	0.2024

<sup>a</sup> Observation criterion  $I > 2\sigma(I)$ ,  $R1 = \sum||F_o| - |F_c|| / \sum|F_o|$ ,  $wR2 = \{\sum[w(F_o^2 - F_c^2)^2] / \sum[w(F_o^2)]\}^{1/2}$ .

range of the ligand field to be covered including that characterized previously by iron(III) phthalocyanines. Such a suitability has been demonstrated here for the representative set of axial ligands. The proposed probe is very sensitive and at present covers the +65.31 to −77.12 ppm paramagnetic shift span (294 K). The demonstrated solvent dependence of the paramagnetic shift may be conceivably used as an additional tool to discriminate fine differences between axial ligands.

## Experimental Section

**Reagents.** The free 2,7,12,17-tetra-*n*-propylporphycene [(TPrPc)-H<sub>2</sub>] was prepared using the reported method.<sup>1</sup> (TPrPc-*d*<sub>4</sub>)H<sub>2</sub> was obtained as previously described.<sup>20</sup> Insertion of iron followed a known route to produce [(TPrPc)Fe<sup>III</sup>]<sub>2</sub>O, which was subsequently cleaved with HX acids to produce (TPrPc)Fe<sup>III</sup>X ( $X = \text{Cl}$ ,  $\text{Br}$ ,  $\text{I}$ ).<sup>12,13,20</sup> The respective sample was dried under vacuum to remove traces of water.

Conversion from the chloride anion to the perchlorate anion followed the published methods.<sup>24,25</sup>

Caution! The perchlorate salts are potentially explosive when heated or shocked. They should be handled in milligram quantities.

Samples of (TPrPc)Fe<sup>III</sup>(C<sub>6</sub>H<sub>5</sub>O) were obtained by addition of an excess of the sodium phenoxide to (TPrPc)Fe<sup>III</sup>Cl in toluene solution, sonication, and filtration to remove sodium phenoxide and sodium chloride following the procedure for an analogous iron(III) porphyrin derivative.<sup>66</sup>

(TPrPc)Fe<sup>II</sup> was obtained by reduction of (TPrPc)Fe<sup>III</sup>Cl in CH<sub>2</sub>-Cl<sub>2</sub> with an aqueous solution of sodium dithionite.<sup>20</sup> Crystals were grown by very slow evaporation of the dichloromethane layer under a water solution of the reducing agent in a closed vial under purified nitrogen in a glovebox.

**X-ray Data Collection and Refinement.** Crystals of (TPrPc)-Fe<sup>III</sup>Cl were prepared by diffusion of hexane into the dichloromethane solution contained in a thin tube.

Crystal data for (TPrPc)Fe<sup>III</sup>Cl and (TPrPc)Fe<sup>II</sup> are given in Table 5, together with refinement details. Both crystals were mounted

onto a glass fiber and then flash-frozen to 100 K (Oxford Cryosystem-Cryostream cooler). Preliminary examination and intensity data collections were carried out on a Kuma KM4CCD  $\kappa$ -axis diffractometer with graphite-monochromated Mo  $K\alpha$  radiation. Crystals were positioned 65 mm from the KM4CCD camera. A total of 612 frames were measured at  $0.75^\circ$  intervals with a counting time of 35 s for (TPrPc)Fe<sup>III</sup>Cl and 30 s for (TPrPc)Fe<sup>II</sup>. The data were corrected for Lorentz and polarization effects. No absorption correction was applied. Data reduction and analysis were carried out with the Kuma Diffraction (Wrocław) programs. The structures were solved by direct methods (program SHELXS97<sup>77</sup>) and refined by the full-matrix least-squares method on all  $F^2$  data using the SHELXL97<sup>78</sup> programs. Disorder exists in the complex (TPrPc)Fe<sup>III</sup>Cl. Molecules have two different orientations (4:1) in the unit cell, but the Fe(1) and Cl(1) atoms have identical coordinates in both cases. These molecules differ by rotation along the Fe(1)–Cl(1) bond by  $90^\circ$ . Non-hydrogen atoms from molecules with primary orientation were refined with anisotropic displacement parameters and isotropically in molecules with secondary orientation using the instruction SAME; coordinates of the hydrogen atoms were calculated using the geometry of the molecules and were refined as riding groups for both orientations of (TPrPc)Fe<sup>III</sup>Cl. In the complex (TPrPc)Fe<sup>II</sup> all non-hydrogen atoms were refined with anisotropic thermal parameters. The carbon-bonded hydrogen atoms were included in the calculated positions and refined using a riding model.

**Magnetization Measurements.** The solid-state magnetization of (TPrPc)Fe<sup>III</sup>Cl and (TPrPc)Fe<sup>III</sup>Br was measured under helium on a Quantum Design MPMS SQUID magnetometer from 2 to 300 K at a field of 0.5 T. The sample was contained in a Kel-F bucket. The bucket was measured independently at the same field and temperatures. The raw data were corrected for the sample holder

(77) Sheldrick, G. M. SHELXS97, program for solution of crystal structures, University of Göttingen, Germany, 1997.

(78) Sheldrick, G. M. SHELXL97, program for crystal structure refinement, University of Göttingen, Germany, 1997.

contribution, and the molar susceptibility corresponds to the resulting magnetization per mole and per magnetic field unit. The diamagnetic contribution of the sample was evaluated using Pascal's constants.

**NMR Spectroscopy.** <sup>1</sup>H NMR spectra were recorded on a Bruker AMX 300 spectrometer operating in the quadrature mode at 300 MHz. The residual <sup>1</sup>H NMR resonances of deuterated solvents were used as a secondary reference.

**Acknowledgment.** Financial support from the State Committee for Scientific Research KBN of Poland (Grant 3 T09A 155 15) and the Foundation for Polish Science is kindly acknowledged.

**Supporting Information Available:** Figures S1–S5, temperature dependence of the <sup>1</sup>H NMR chemical shifts of some protons for (TPrPc)Fe<sup>III</sup>(ClO<sub>4</sub>), (TPrPc)Fe<sup>III</sup>Cl, (TPrPc)Fe<sup>III</sup>Br, (TPrPc)Fe<sup>III</sup>I, and (TPrPc)Fe<sup>III</sup>(PhO), Figure S11, various views of (TPrPc)Fe<sup>III</sup>-Cl, Table S11, crystal data and structure refinement for (TPrPc)Fe<sup>III</sup>Cl, Table S12, atomic occupancy factors, coordinates, and equivalent/isotropic displacement parameters ( $\text{\AA}^2$ ) for (TPrPc)Fe<sup>III</sup>-Cl, Table S13, bond lengths ( $\text{\AA}$ ) and angles (deg) for (TPrPc)Fe<sup>III</sup>-Cl, Table S14, torsion angles (deg) for (TPrPc)Fe<sup>III</sup>Cl, Table S15, lengths ( $\text{\AA}$ ) and angles (deg) of the hydrogen bonds for (TPrPc)Fe<sup>III</sup>Cl, Table S16, least-squares planes for (TPrPc)Fe<sup>III</sup>Cl, Figure S21, various views of (TPrPc)Fe<sup>II</sup>, Table S21, crystal data and structure refinement for (TPrPc)Fe<sup>II</sup>, Table S22, atomic occupancy factors, coordinates, and equivalent/isotropic displacement parameters ( $\text{\AA}^2$ ) for (TPrPc)Fe<sup>II</sup>, Table S23, bond lengths ( $\text{\AA}$ ) and angles (deg) (TPrPc)Fe<sup>II</sup>, Table S24, torsion angles (deg) (TPrPc)Fe<sup>II</sup>, and crystallographic data in CIF format. This material is available free of charge via the Internet at <http://pubs.acs.org>.

IC010725J